

## **A Real Challenge in Mine Water Management in a High Precipitation Area: Grasberg Mine**

**Nanda Rinaldi**, PT Freeport Indonesia, Indonesia

**Iwan Setiawan**, PT Freeport Indonesia, Indonesia

**Vladimir Ugorets**, SRK Consulting (US), Inc., USA

**Göktuğ Evin**, SRK Consulting (US), Inc., USA

### **Abstract**

The Grasberg Mine is the world's largest gold mine, and is also one of the largest copper producers in the world. The mine poses a real challenge for hydrogeologists due to its size and complex hydrogeological setting, including structurally controlled groundwater flow. The mine sits in a mountainous area with rainfall of up to 5 m per year. The site geology features highly undulated sedimentary rocks and vertical intrusions hosting the mineralization. Karstification exists in the area and influences structural control of the groundwater flow path in the vicinity of the open pit and underground mines.

The applied mining method for the Grasberg intrusive complex (GIC) also complicates water management. The existing open pit is approximately 1.5 km deep and a block cave operation is under development approximately 400 m below the pit bottom. Block caving will propagate to the pit bottom eventually and will create a highly transmissive cave zone, which will connect drawpoints to the bottom of the open pit.

Near the GIC, the East-Ertsberg skarn system (EESS) has been mined since 1982 by systems of five vertical block caves (GBT1, GBT2, IOZ, DOZ, and DMLZ). The implemented dewatering systems for both the GIC and EESS areas, with a total flow of approximately 41,000 gallons per minute (gpm) or 2.6 m<sup>3</sup>/s, allows lowered water levels in the vicinity of the open pit and underground mines by discharging groundwater via gravity by a system of upward drainholes drilled from the underground drifts.

To assist in the development of dewatering and mine water management strategies for the remaining life of mine, a comprehensive groundwater flow model was developed by using the finite-element *MINEDW* code and calibrated to the available flow and water level data collected over a 20-year period of active mining.

## Hydrogeological Conditions

The Grasberg Mine is located in Papua, Indonesia in a mountainous area where a rainfall of up to 5 m per year is subject to El Niño’s periodic occurrence. The site geology is extremely complex with highly undulated sedimentary rocks and vertical intrusions hosting the mineralization. Karstification exists in the area and influences structural control of the groundwater flow path in the vicinity of the open pit and underground mines.

## Regional Hydrogeology

The regional geologic framework of the Grasberg minerals district consists of a series of folded and faulted carbonate and sandstone units that range from about 700 to 3,000 m in thickness. These formations have relatively low permeability unless karstified or fractured. The maximum thickness of the formations occurs along the Yellow Valley syncline near GIC, and to the north of the EESS as shown in Figure 1.

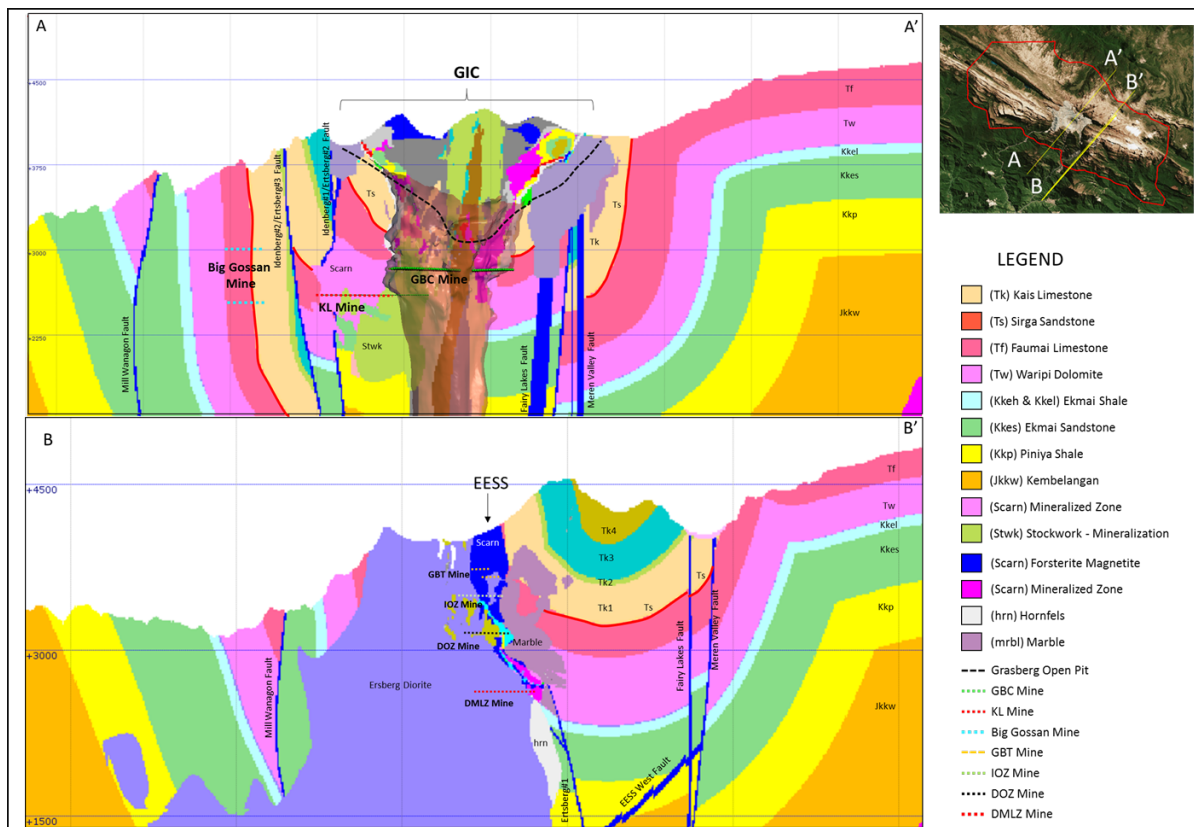


**Figure 1: Geology of Grasberg and EESS mines shown with cross-sections**

The Grasberg Mine complex is located at the intersection of two major structural systems: NW/SE-trending faults that are parallel to the axis of the Jayawijaya Mountains, and NE/SW-trending cross-faults, normal to the axis of the mountains. The Idenberg #1 and #2, Fairy Lakes, and Meren Valley and axial

faults and the Grasberg, Carstensch and New Zealand Pass cross faults are major water-bearing features in vicinity GIC and EESS.

Within the Grasberg area, the most important and permeable water-bearing units are: the Poker Chip Zone (currently mined out); the fractured upper part of the Kali intrusive; the Heavy Sulphide Zone (HSZ) contacts between the sedimentary units and the GIC; and Grasberg, Idenberg#1 and Carstensch faults.

The near-surface limestone units are often karstified to depths of 300 m below ground surface and significantly deeper along major structures. The karstic features in the limestone provide permeable conduits for groundwater flow as confirmed by a series of tracer tests. There are three major known karstic sinkholes/features: Carstenschweide (CST) with two sinkholes to the north of the GIC and Yellow Valley with one sinkhole to the north/northeast of the EESS.

The ore within the EESS occurs within a skarn that formed at the contact between the Ertsberg diorite intrusion and the primary limestone country rock. Mining of the DOZ started in late 2000 by block caving similar to the previous block caving in the overlying GBT I, GBT II and IOZ mines. The cave propagated to the surface in a portion of the eastern half of the DOZ mine and up to the IOZ cave in the western part of the DOZ and formed a combined GBT/IOZ/DOZ cave. Mining of the DMLZ started in 2015 by block caving at an elevation of 2,600 mamsl (meters above mean sea level) (or approximately 500 m below the DOZ level) and a combined GBT/IOZ/DOZ/DMLZ cave zone would be formed.

Within the EESS area, key preferential pathways of the groundwater are: diorite at an elevation above about 3,400 mamsl, West Fault Zone, and Guru, Ertsberg #1 and Cave faults. As the DOZ/DMLZ cave and crack limits expand through time into these units, they will contribute lateral residual passive inflow directly to the cave zone.

### **Groundwater Recharge and Discharge**

Recharge of precipitation is a major stress to the groundwater system and varies significantly across the HSA (hydrogeological study area). Recharge of surface water into the groundwater system occurs predominantly through sinkholes in the karstic limestone or through areas with outcrops of more permeable intrusive rocks. Figure 2 shows the location of 19 rainfall stations installed within the HSA. Rainfall stations are located at elevations ranging from 3,100 to 4,544 mamsl in the Upper Wanagon to the west of the GIC (northwest of the proposed KL block cave). Data from the stations are available from 1995 through 2017. The rainfall data define the following two major areas with different precipitation rates (Figure 2):

- High elevation (15 stations) with average precipitation ranges from 9.1 to 10.9 mm/d (long-term average rate of 9.8 mm/d); and

- Southern slope (4 stations) with average precipitation ranges from 13.2 mm/d to 16.3 mm/d (long-term average rate of 15.0 mm/d). It is envisaged that the topographical divide at the southern part of the HSA acts as a boundary to the S-N trending winds. Therefore, precipitation condenses at the southern part of the divide.

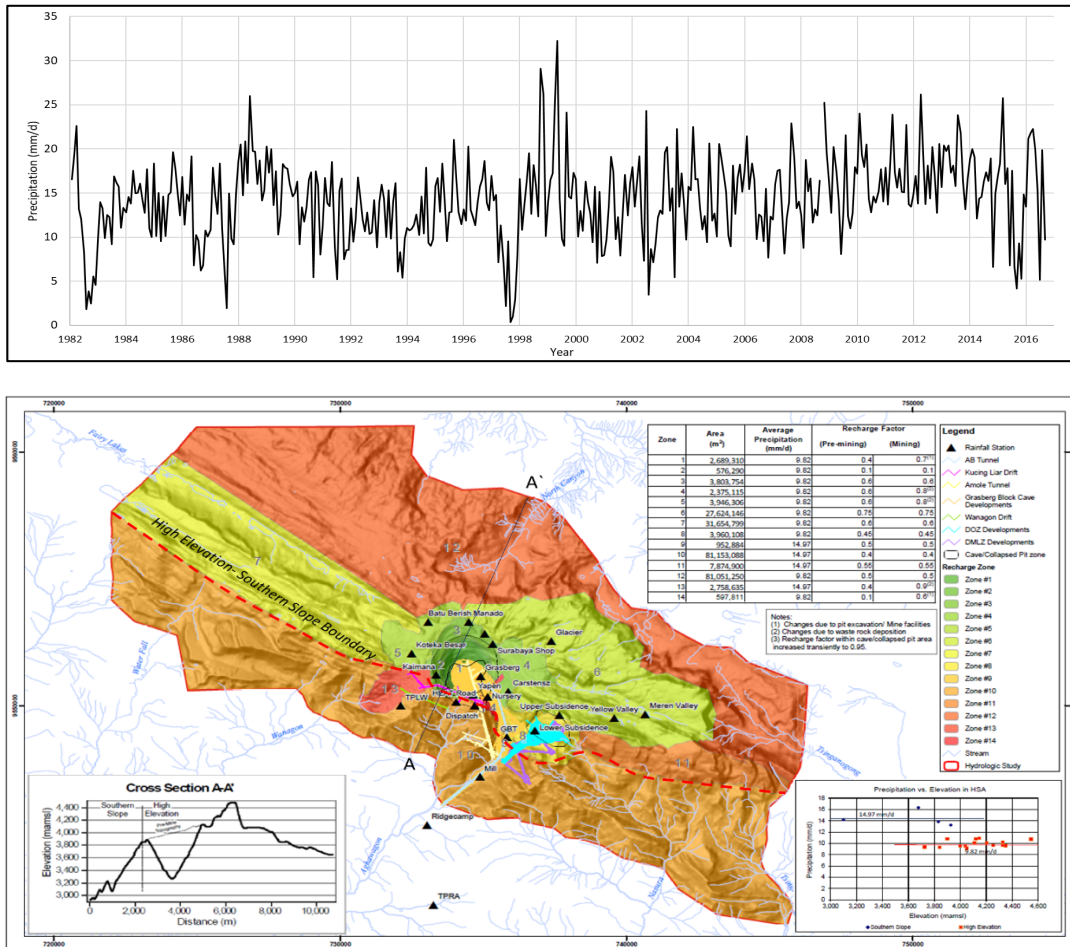


**Figure 2: Location of rainfall stations, distribution of precipitation zones and recharge factors and historic precipitation data**

Figure 2 shows historic monthly averaged precipitation rates for Mill station with the longest (from 1982) record indicates large variation in rainfall and the impact of strong El Niño events (in 1982, 1987, 1997, 2003, and 2015). The maximum measured monthly average precipitation is 32.3 mm/d (Mill, April 1999) and minimum measured monthly average precipitation is 0.08 mm/d (Yellow Valley, September 1997). The wettest conditions occur in December through April and relatively dry conditions occur in June through August.

As much as 75% of the precipitation is estimated to recharge the groundwater system in these closed alpine karst basins. Recharge in the non-karstified areas is estimated to range from 60% in areas underlain

by limestone to 10% to 45% in areas underlain by intrusive rocks as shown in Figure 2. This distribution is based on analyses of slope, presence of surface water outflow and hydraulic parameters. Recharge factor values were verified in the process of model calibration.

Groundwater in the HSA eventually discharges into one of nine major streams. However, both major and minor faults and related structures allow groundwater to flow beneath topographic divides, at least at the sub-basin level. Additionally, groundwater discharge occurs as springs along beds of low permeability rock. Most of these springs occur at an elevation of about 3,300 mamsl, probably at the base of the alpine karst system. These springs comprise the headwaters of most of the perennial streams.

Generally, the regional groundwater flows from the topographic highs at the watershed divide toward areas of lower elevation in the south or southeast. Intrusive complexes generally show low permeability, and tend to be hydraulic barriers to the groundwater flow generated by meteoric recharge in the Jayawijaya Mountains.

### **Groundwater Inflow Management**

Figure 3a shows the locations of groundwater intersections by drifts and drillholes, and locations of flow measurement stations.

Groundwater flow in the GIC area discharges into the Amole drift with maximum measured flow up to 12,000 gpm from drainholes installed in the northern part of the drift (above X/C #17). During excavation of the open pit, significant inflow was not observed (the maximum observed inflow in the north-eastern segment of the pit did not exceed 1,500 gpm) due to efficient groundwater capturing from the Amole drift below.

Current groundwater inflow to the Grasberg Block Cave (GBC) development is about 4,000 gpm. The majority of inflow is observed along the contacts between the Karume and Kali intrusives and the carbonate rocks. A series of hydraulic tests from Amole piezometers to the GIC indicate that the GIC rocks generally are of low permeability except where fractures/structures exist.

The cave will break through to the bottom of the pit during mining of the GBC and the cave and crack zones will propagate into the walls of the Grasberg Pit. Due to its location below the Grasberg Pit, rainfall within this area infiltrates and enters the proposed GBC and KL (Kucing Liar) mines.

Groundwater flow in the DOZ mine discharges into MLA drift and partially through DOZ pipe. Total mine discharge (inflow to drillholes, drifts and draw points) was in the range of 10,000 to 12,000 gpm (MLA flow is up to 8,000 gpm) when measured from 2004 through 2013. Groundwater intersections have occurred starting in 2014 in DMLZ developments (water discharges into AB tunnel) with total flow of up to 10,000 gpm, resulting in decreased MLA flow from 8,000 to as low as 3,000 gpm. This decrease indicates a good hydraulic connection between the DOZ and DMLZ mines.

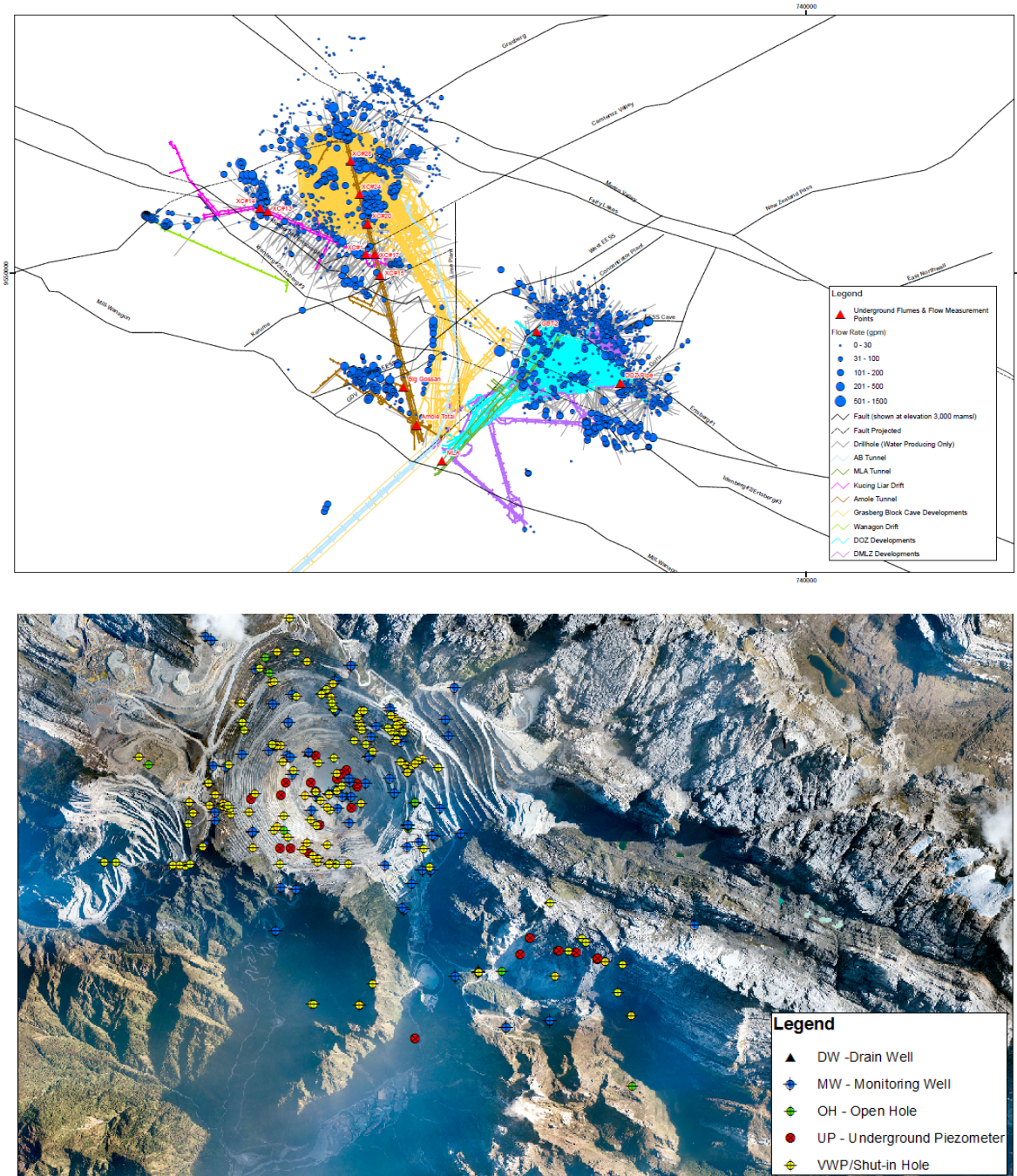


**Figure 3: Location groundwater intersections by drainholes, flow measurement stations (a), and piezometers with water level measurements (b)**

### Groundwater Level Distribution

Figure 3b shows locations of monitoring wells with measured water levels.

Prior to mining and dewatering of the Grasberg Pit and based on anecdotal evidence, the groundwater levels in the GIC and surrounding limestone were about the same. As a result of drilling underground drainholes into the contact zones on both sides of the HSZ, water levels in the GIC and

contact zones have decreased significantly while the water levels in the surrounding limestone have been dropping at a much slower rate. Water level declines in the surrounding limestone have occurred only in areas near the HSZ contact or close to the dewatering drainholes. Piezometers in south, east and northeast limestone showed a small amount of drawdown, while those in the north and northwest of the HSZ remained high. The lack of drawdown is attributable to the ring of low permeability limestone/marble below the hinge point of the wineglass-shaped GIC.

Measured water levels in the underground piezometers installed within the lower part of the GIC stand at 2,855 to 3,108 mamsl (i.e., about 35 to 288 m above the GBC mining area). Most of these piezometers are artesian holes with measured water levels between 8 and 12 m above the Amole drifts. Although the pressure heads are above the Amole drift level, the flows are small, which confirms that the GIC rock is of low permeability and likely extends to the GBC level.

Measured water levels in the EESS area are limited and measured in the range from 3,440 to 3,150 mamsl (DOZ level) and from 3,1000 to 2,585 mamsl (DMLZ level) in underground piezometers within the north wall sedimentary rock. Water levels in the surface piezometers are measured within fractured diorite (from 3,808 to 3,426 mamsl) and about 3,700 mamsl in Yellow Valley syncline.

All water level measurements indicate a presence of downward hydraulic gradient due to groundwater intersections from underground developments and low permeability of the rock.

## **Description of Groundwater Flow Model**

The numerical model was developed to predict groundwater inflows to existing and being constructed block cave mines. The model was constructed by using the *MINEDW* finite-element code, which is specially designed to model mine dewatering projects. Some key features of this code – collapsing grid to simulate open pit excavation, non-linear flow in the drains intersecting large groundwater flow in the permeable faults, modeling of permeable faults by additional linking nodes with additional transmissivity, changes hydraulic conductivity in time to simulate cave/crack line propagations – were specially designed to model groundwater flow in the vicinity of the Grasberg open pit and EESS block cave mines (Azrag et al., 1998; Ugorets, 2016).

The three-dimensional finite-element grid of the model contains 175,716 nodes and 328,797 elements in 17 numerical layers and encompasses an area of about 251 km<sup>2</sup> within nine surface water basins, covers in detail the existing and future mines and are shown in Figure 4.

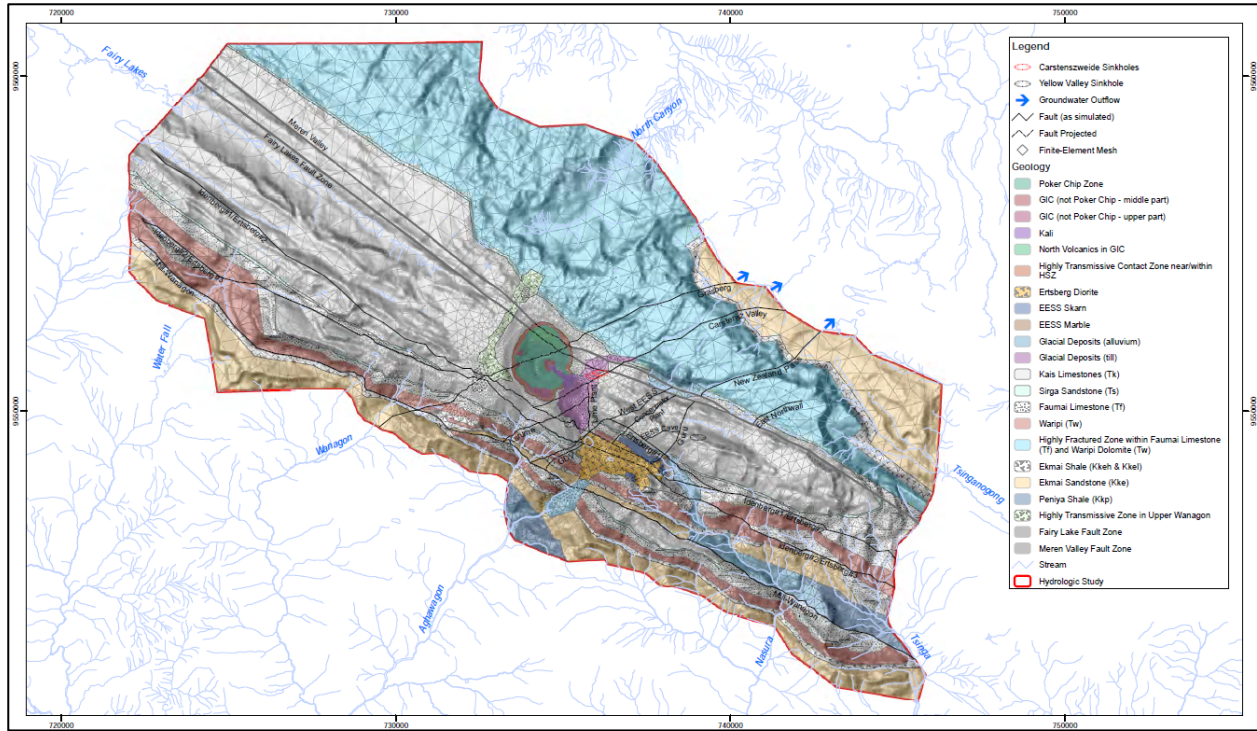


**Figure 4: Plan view of finite-different mesh of model shown simulated geology in uppermost layer and faults**

### Simulation of Hydrogeology

Sixty-two hydrogeologic zones with various hydraulic parameters were incorporated into the model and simulated, generally decreasing hydraulic conductivity values with depth. Hydrogeologic zones in cross section A-A' through the Grasberg and KL areas are shown in Figure 10a before excavation of the open pit when the open pit will be fully excavated and when Grasberg and KL block caves will be completed. Hydrogeologic zones in cross section B-B', through the EESS area, are shown on Figure 10b a for pre-mining conditions and at the end of DMLZ block caving.

The hydraulic conductivity tensor has been rotated with respect to the model grid such that  $K_{xx}$  is oriented at an azimuth of  $117^{\circ}$  (or  $N63^{\circ}W$ ), parallel to the trend of the Jayawijaya Mountains and the associated fold axes. Some of the hydrogeologic units (e.g., all intrusive and metamorphic rocks) simulated isotropic, but most of the sedimentary units have been made anisotropic with the general relationship  $K_{yy} \geq K_{xx} \geq K_{zz}$ . This anisotropy is used to represent the effects of the major joint system and small faults.

### Simulation of Faults

The 17 major faults are incorporated into the model by linking two nodes with very high transmissivity between them. The horizontal traces of the nodes linked to represent the various faults are indicated in

Figure 4. The vertical traces of the nodes linked to represent the various faults are shown in the two cross sections of the model in Figures 5 and 6. There are 22,776 pairs of such linked nodes in the model. Two major regional faults to the north from GIC (Meren Valley and Fairy Lakes) were simulated by a system of narrow elements with high hydraulic conductivity and low storage parameters.

### **Simulation of Recharge from Precipitation**

Recharge from precipitation is assigned by multiplying recharge factors by rainfall rates within two precipitation zones (both shown in Figure 2).

Monthly average data for each precipitation zone were obtained by averaging available data starting in 1995 from rain stations within each area. Prior to 1995, data from Mill station (available from 1982) were used to reproduce precipitation within these two zones by multiplying Mill precipitation records by coefficients of 0.691 and 1.004. These two coefficients represent the relationship between estimated average precipitations for these two zones to the Mill average rainfall value.

Long-term average precipitation data were used for pre-mining steady-state and predictive transient simulations. Monthly precipitation was used to apply recharge during transient calibration (from 1982 through 2016).

### **Simulation of Underground Workings and Groundwater Intersections**

The underground workings and associated dewatering systems are presented in the model as drifts and drillholes. They are incorporated into the model by specific drain nodes with time-variable leakance factors depending on a difference between water level and an elevation of mine development (Azrag et al., 1998; Ugorets, 2016). Using this approach allows more realistic simulation of high water discharge by drainholes drilled into the transmissive faults.

Groundwater flow near discharge points in fractured and faulted rock is usually non-Darcian, and the standard groundwater flow equation breaks down in describing such flow (Dudgeon, 1985). To account for this non-Darcian flow, authors used the non-linear flow algorithm of *MINEDW* (HCI, 1993), which include both linear and non-linear coefficients from the Forchheimer equation.

All drainholes and parts of the drifts that have intercepted a significant amount of water (i.e., greater than about 50 gpm) are simulated in the model by drain nodes with head dependent leakance factors and considering non-Darcian flow. They are represented by a series of 3,876 model drain nodes.

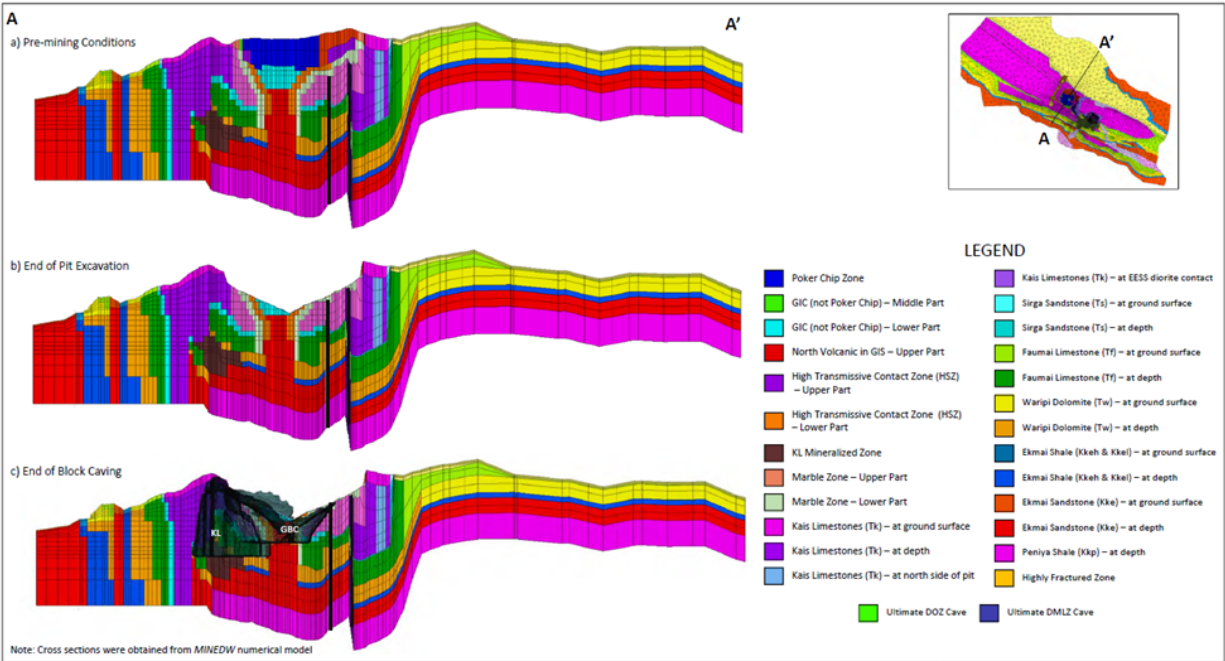


Figure 5: Model cross-section through Grasberg area

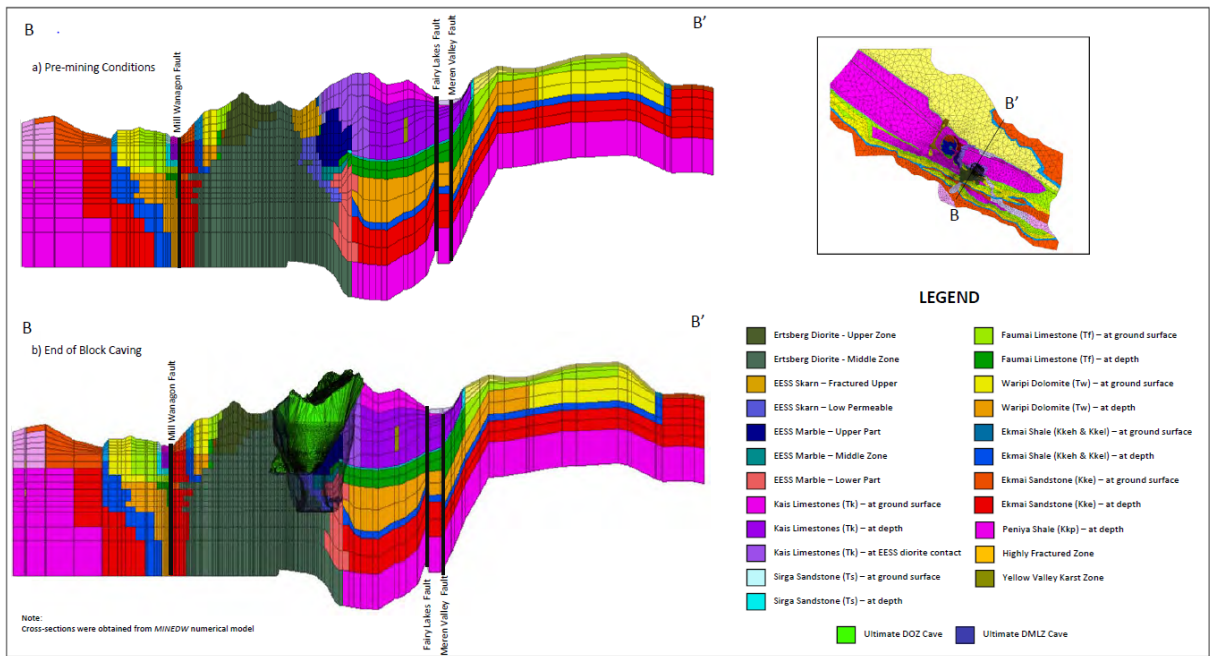


Figure 6: Model cross-section through EESS area

### Simulation of Open Pit

The excavation of the Grasberg Pit is simulated by pit nodes with a collapsing grid inside the pit area. This was done by the changing of the elevations of the nodes at the top of the first layer within the pit area to the specified pit elevation. The hydraulic properties within the area of the collapsing grid are adjusted

to the appropriate values as the grid collapses, to simulate mining. Annually pit plans from 1996 to 2018 were incorporated into the model using linear monthly interpolation. The final elevation of the bottom of the Grasberg Pit was assumed to be 3,085 mamsl. The collapsed grid for the final Grasberg Pit is shown in the model cross section in Figure 5.

A zone of relaxation around the excavated open pit was simulated by automatically assigning elements below the pit nodes at the appropriate time. The hydraulic conductivity of this approximately 50 m wide zone is assumed to be 0.1 m/day.

### Simulation of Block Caves

The EESS, GBC and KL block caves are simulated by:

- Assigning relatively large values of hydraulic conductivity to the cave and fractured zones ( $K=1$  m/d and  $K=0.1$  m/d, respectively), and
- Increasing the assigned recharge factor over the area where the cave limit is predicted to propagate to the ground surface from the original value in that area (which ranges from 0.1 – 0.75 to 0.95).

Historic and future propagations of the EESS cave and fractured zone limits (shown in Figures 6 and 7) observed and estimated by geotechnical models were incorporated into the model. Future propagations of GBC and KL BC were simulated similarly.

Although development of the cave and fractured zones will be essentially continuous in time, it is simulated in the model in different discrete stages.

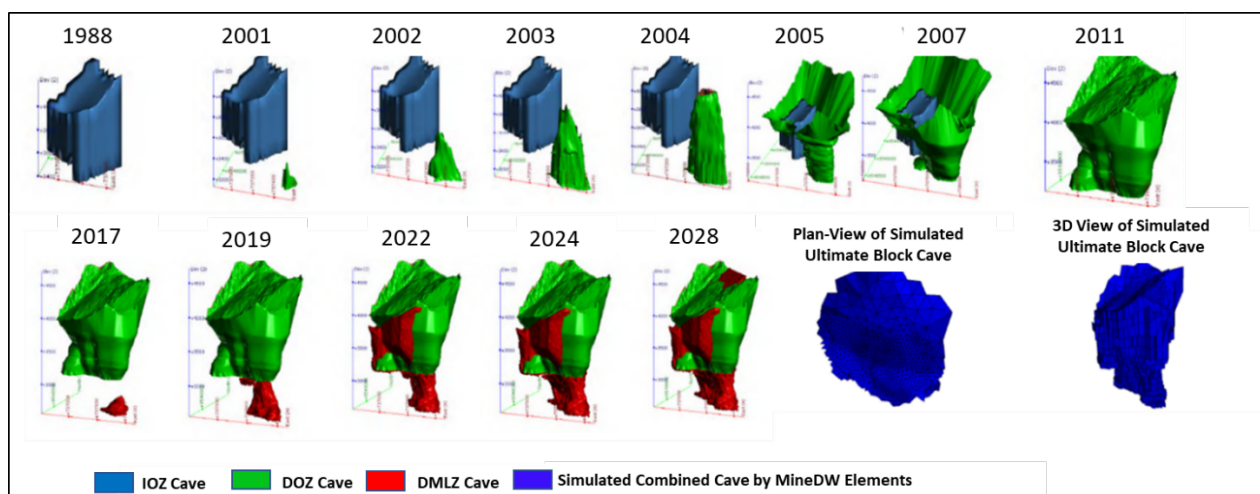


**Figure 7: Simulated propagation of IOZ, DOZ, DMLZ cave zones in time**

## Model Calibration and Predictions

The model was calibrated to groundwater flows intersected by underground drainholes and measured water levels in time. As example, comparison of measured and calibrated total flows at the portals of dewatering drifts is shown in Figure 8. Calibrated model to transient conditions was used for predicting groundwater inflows to proposed block caves and total flows at the portal of dewatering drifts. Their results are shown in Figure 9.

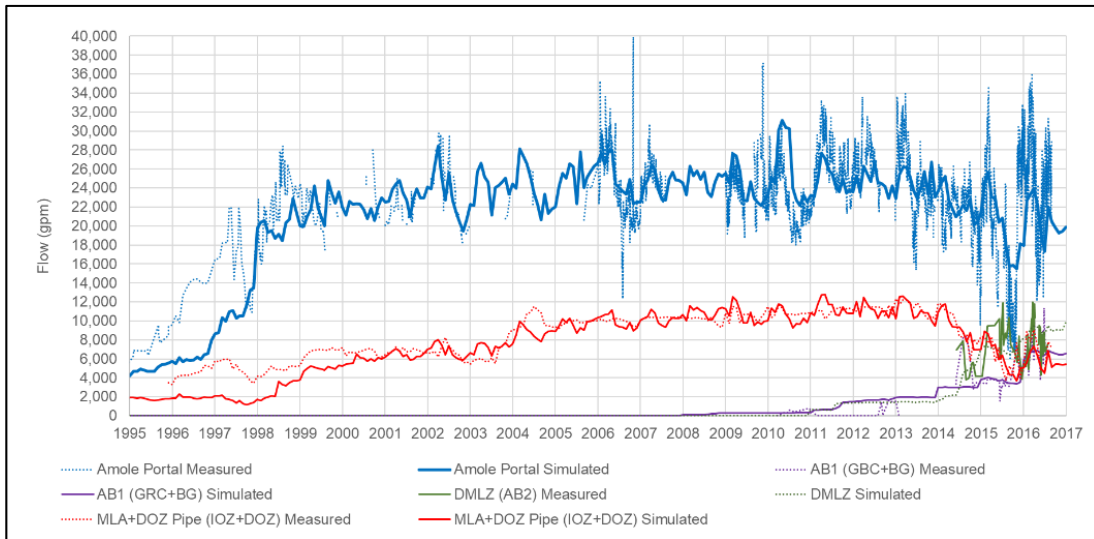


**Figure 8: Results of model calibration to measured flows in dewatering drifts**

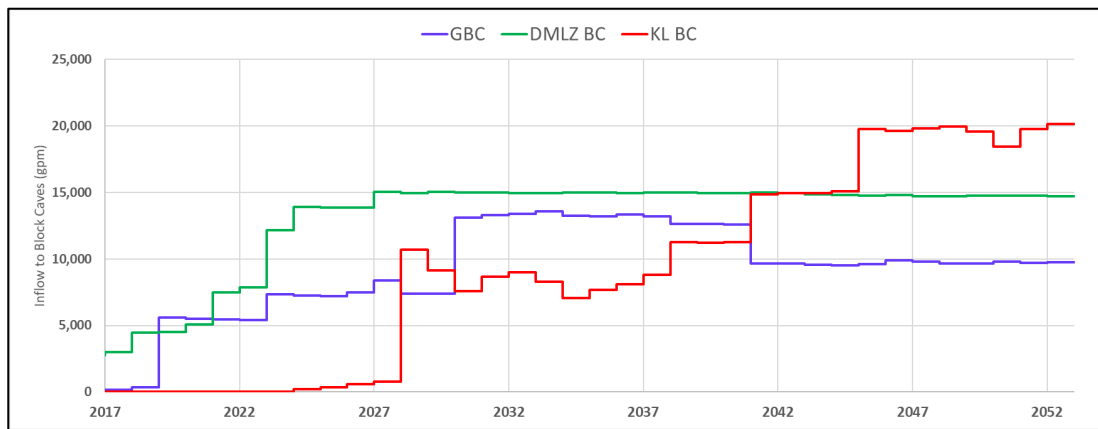


**Figure 9: Predicted inflows to GBC, DMLZ, and KL Caves**

Maximum predicted inflow to block caves simulated under long-term precipitation conditions and Base Case scenario of cave/crack zone propagation are:

- GBC – 12,800 gpm (or 0.8 m<sup>3</sup>/s);
- DMLZ – 15,000 gpm (0.95 m<sup>3</sup>/s);

- KL BC –20,000 gpm (or 1.26 m<sup>3</sup>/s); and
- Total mine discharge to block caves and ancillary drifts –56,700 gpm (or 3.57 m<sup>3</sup>/s).

Predictions of the water table at the end of mining indicate that these three block caves will locally create very steep “cone of depression” around the mines.

## Conclusions

Challenges in mine water management in high precipitation areas of the Grasberg Mine posed by complex hydrogeological and mining settings were addressed during the comprehensive conceptualization and numerical modeling processes, including:

- Development of conceptual hydrogeological models of individual mine areas, including complex lithology and presence of transmissive structures with spatial contrasts (up to three orders of magnitude) in hydraulic conductivity distribution.
- Extremes in recharge rates from precipitation and their drastic variability in time and space.
- Presence of karstic zones (sinkholes) and highly permeable faults with non-linear flow conditions.
- Simulation groundwater discharge to drainholes and underground developments by drain nodes with head-dependent leakance factors and considering non-Darcian flow.
- Handling of large amounts of monitoring data (groundwater flows and water levels) with model calibration to more than 20 years transient mining conditions.
- Simulation of complex mining developments including the Grasberg Pit with dynamic changes in open pit elevation and propagation of ZOR around the pit, GBC block cave operation below ultimate Grasberg Pit, and five stages of cave and fractured zone propagations in the EESS (from GBT1, GBT2, IOZ, DOZ, and DMLZ block caves) required detailed handling of transient hydraulic parameters modification in space.
- Using specialized finite-element groundwater modeling *MINEDW* code allowed for the simulation of the items described below (this code was modified by developer several times during process of the modeling by author requests), and minimized numerical problems in the process of the transient simulations.

The results of the predictive numerical simulations and conducted sensitivity analysis indicate that the propagation of the cave zone and associated crack limit into the carbonate rock (and intrusive rock for EESS) is the most sensitive parameter with respect to predicted inflows to the block caves. Cave material and adjacent highly fractured rock propagates toward the ground surface and intersects the permeable shallow groundwater system. Inflow to the block caves also depends on transmissivity of the faults

intersecting the block cave and hydraulic conductivity of marble zones that limit groundwater inflow to the cave.

The numerical model predicts that the groundwater system at the end of mining will reach near-steady-state conditions and total flow in the AB, Amole, and MLA portals will remain at a rate of about 56,700 gpm during post-mining conditions.

## References

- Azrag, E.A., Atkinson, L.C. and Ugorets, V.I. 1998. Use of a finite element code to model complex mine water problems, in *Mine Water and Environmental Impacts*, Proceedings of the International Mine Water Association Symposia, Johannesburg, South Africa, Vol. 1: 31–41. Johannesburg: International Mine Water Association.
- Dudgeon, C.R. 1985. Effect of non-Darcy flow and partial penetration on water levels near open-pit excavation, Hydrogeology in the service of man, *Memoires of the 18th Congress of the International Association of Hydrogeologists*, Cambridge, XVIII(4): 122–132.
- HCI. 1993. MINEDW – a finite element program for three-dimensional simulation of mine dewatering, unpublished report. Hydrologic Consultants, Inc.
- Itasca International Inc. 2016. *MINEDW 3.0 User Manual*.
- Ugorets, V.I. 2016. Benefits of MINEDW code for mine dewatering projects in complex hydrogeological settings, in *Proceedings of 4th Itasca Symposium on Applied Numerical Modeling in Geomechanics*, March 7–9, 2016, Lima, Peru, pp. 509–518.